International Journal of Mass Spectrometry 290 (2010) 85–93

Contents lists available at ScienceDirect

International Journal of Mass Spectrometry

journal homepage: www.elsevier.com/locate/ijms

Mass spectrometry of hydrogen bonded clusters of heterocyclic molecules: Electron ionization vs. photoionization

Viktoriya Poterya[a], Ondřej Tkáč[a,1], Juraj Fedor[a], Michal Fárník[a,*], Petr Slavíček[b,2], Udo Buck[c]

[a] J. Heyrovský Institute of Physical Chemistry, v.v.i. Academy of Sciences of the Czech Republic, Dolejškova 3, 18223 Prague 8, Czech Republic
[b] Department of Physical Chemistry, Institute of Chemical Technology, Technická 5, 16628 Prague 6, Czech Republic
[c] Max-Planck Institut für Dynamik und Selbstorganisation, Bunsenstr. 10, D-37073 Göttingen, Germany

ARTICLE INFO

Article history:
Received 21 October 2009
Received in revised form 3 December 2009
Accepted 3 December 2009
Available online 16 December 2009

Keywords:
Cluster photochemistry
Hydrogen bonded cluster
Heterocyclic molecule
Molecular beam
Dynamics

ABSTRACT

Clusters of small heteroaromatic ring molecules pyrrole, imidazole and pyrazole were studied in a molecular beam experiment. Neutral cluster size distributions under various expansion conditions were probed by a scattering experiment with a He-atom beam. The clusters were ionized by electrons and their mass spectra were measured by a quadrupole mass spectrometer. Alternatively, the ionization was achieved by a non-resonant subsequent multiphoton process with 193 nm photons and the time-of-flight mass spectra were recorded. (1) The differences in the methods of cluster ionization, namely subsequent multiphoton and single photon ionization, and electron ionization are discussed. (2) More importantly, the differences between the ionization of pyrrole clusters on the one side, and imidazole and pyrazole clusters on the other side are studied. The existence of larger protonated fragments in the latter spectra points to a higher photostability in these N–H···N hydrogen bonded systems as opposed to the more weakly N–H···π bound pyrrole clusters. The experiments are accompanied by *ab initio* calculations supporting and interpreting the experimental results.

1. Introduction

Mass spectrometry offers a variety of tools for investigations of biological molecules. Recently, it was demonstrated, that ultraviolet light can be utilized to initiate unique and potentially useful fragmentation in peptides and proteins [1]. In this respect, the study of weakly bound molecular clusters upon ionization can shed some light on the behavior of the biological molecules. Constituents of biomolecules can be prepared in a supersonic beam either surrounded by solvent molecules or forming molecular aggregates. The size of the clusters can be varied by changing the expansion conditions and the type of weak interaction can be tailored by choosing appropriate molecular systems. The dynamical processes following the ionization are often dramatically altered upon the complexation with some channels closing and various new reaction channels opening at the same time. By the way of example, in benzene clusters a dimer ion core is formed [2,3] while in hydrogen bonded systems the donor proton is typically transferred to the acceptor molecule, e.g., in the case of water [4]. Such environmentally induced processes are important for example in oxidative DNA damage or charge transfer in nucleic acids.

In this study, we have investigated different ionization processes for molecular clusters composed of small nitrogen-containing ring molecules: pyrrole (Py), imidazole (Im) and pyrazole (Pz). These molecules constitute elementary building blocks in the larger biological species. For example, the pyrrole structure is present in hemes and chlorophylls, the imidazole structure can be found in purine or as the side chain of the naturally occurring amino acid histidine.

Ionization of the gas phase pyrrole [5,6] and imidazole [7], as well as the imidazole in water environment [8] was studied previously. Ionization of the clusters of these molecules was explored to a much lesser extent [9].

Despite their similarities as isolated molecules, pyrrole, imidazole and pyrazole clusters are bound via different types of bonding. The different bonding motifs are represented for the dimers and trimers in Fig. 1. In the pyrrole clusters the N–H bond of one molecule binds to the π electron cloud of the neighboring molecule, the N–H···π bond. Imidazole molecules bind via a standard N–H···N hydrogen bond, while the two pyrazole molecules in the dimer interact via a double hydrogen bond. In the two latter cases, one could expect hydrogen (or proton) migration once the cluster is excited or ionized. For all clusters, the intermolecular interactions are relatively strong.

* Corresponding author. Tel.: +420 266053206; fax: +420 286582307.
E-mail addresses: michal.farnik@jh-inst.cas.cz (M. Fárník), petr.slavicek@vscht.cz (P. Slavíček).
[1] Also at: Faculty of Mathematics and Physics, Charles University in Prague, Czech Republic.
[2] Also at: J. Heyrovský Institute of Physical Chemistry, Academy of Sciences of the Czech Republic, Czech Republic.

1387-3806/$ – see front matter © 2009 Elsevier B.V. All rights reserved.
doi:10.1016/j.ijms.2009.12.007

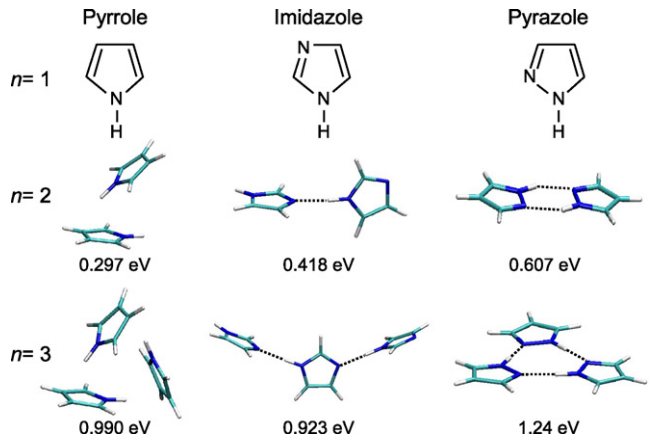

Fig. 1. Structures of the molecules and the different bonding motifs represented by the pyrrole, imidazole and pyrazole dimers and trimers. Hydrogen bonds are indicated by the dashed lines. The structures and binding energies were calculated at the MP2 level using aug-cc-pVDZ basis set.

We address here the question how are the dynamical processes following the ionization of the cluster controlled by the ionization method. We compare the electron ionization (EI) and subsequent non-resonant ultra-violet multiphoton ionization (UVMPI) measured in this study, and also a single photon ionization of the corresponding molecules found in the literature [5,7]. The non-resonant multiphoton ionization turns out to be quite different from both the electron ionization and from a single-photon ionization. Due to the delay between the subsequently absorbed photons the ionization products reflect not only the ionization dynamics but also the dynamics upon the photoexcitation. We therefore argue here that the UVMPI method can serve also as a tool for the study of photodynamics, in a similar fashion as we have recently used the multiphoton photodissociation to study vibrational cooling of the photoexcited acetylene [10].

The photodynamics of the isolated nitrogen heterocycle molecules is reasonably well understood, based on extensive experimental studies [11,12,7,8] and theoretical calculations [13–16]. Briefly, the dissociation of the N–H bond via the $\pi\sigma^*$ state was identified as a major deactivation pathway at lower wavelengths while internal conversion via $\pi\pi^*/S_0$ conical intersection seems to become more important at larger photon energies. We have recently studied the various effects, which the solvation and hydrogen bonding in clusters can have on the photodissociation dynamics of pyrrole [17] and imidazole [18]. We have concluded that the $\pi\sigma^*$ dissociation channel is suppressed upon the complexation both for pyrrole and imidazole, even though the mechanisms of closing this reaction channel is somewhat different for these two molecules.

Mass spectrometry (utilizing the electron ionization and scattering experiments) served in our photodissociation experiments (i) to determine the neutral cluster size distribution, and (ii) to reveal information about the ionization mechanism in the clusters [9]. Here we concentrate on the ionization process itself and extend the previous studies into several directions. First, we directly compare ionization in various clusters which are weakly bound in different ways. Second, we compare various methods of ionization, namely the subsequent non-resonant ultra-violet multiphoton ionization. By using this technique, we show different degree of photostability of the studied clusters, with hydrogen bonded clusters (imidazole, pyrazole) being stabilized as opposed to pyrrole clusters.

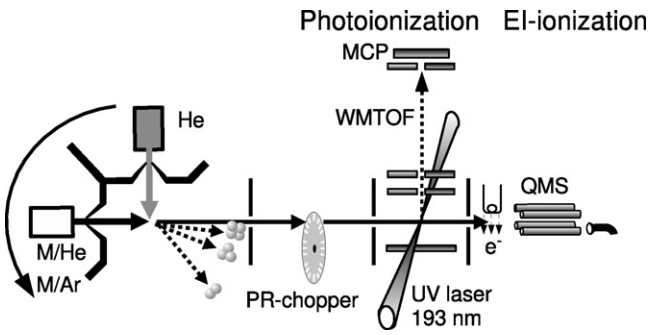

Fig. 2. Schematic picture of the experimental apparatus.

2. Experiment

The experimental apparatus was built and used previously in the Max-Planck Institute in Göttingen [19–22], and moved to the J. Heyrovský Institute in Prague. The schematic picture of the apparatus is shown in Fig. 2.

The clusters are produced by a supersonic expansion through a conical nozzle 55 μm in diameter, 2 mm long, and 30° opening angle. Liquid pyrrole was kept at a constant temperature T_R in a reservoir outside the vacuum chamber and the pyrrole molecules were carried to the nozzle with the carrier gas passing through the reservoir at a constant pressure. Imidazole and pyrazole are solids at room temperature and atmospheric pressure. Therefore a new beam source has been designed and built for producing clusters of molecules from solid samples with sufficiently high vapor pressures at moderate temperatures. It consists of a reservoir oven heated to a constant temperature T_R inside the vacuum chamber. The carrier gas passes through the reservoir containing the sample and the vapor mixture is carried to the nozzle through a 90 mm long stainless-steel tube with 3 mm inner diameter. The tube and the nozzle are heated separately from the reservoir to a somewhat higher temperature T_0 (typically by 20 K) to prevent condensation in the nozzle. In the present experiments Ar or He were used as carrier gases, and T_R and T_0 were varied, in order to produce different cluster size distributions. The concentration of the molecules in the carrier gas was determined from the vapor pressure at the temperature T_R according to the thermochemical data for pyrrole [23] and for imidazole and pyrazole [24]. Selected expansion conditions are summarized in Table 1.

After passing through a skimmer followed by two differentially pumped vacuum chambers the cluster beam enters a transversely mounted Wiley–McLaren time-of-flight mass spectrometer (WMTOF). In the extraction region of the WMTOF the clusters interact with the UV photons and are ionized by a non-resonant multiphoton process and the ion fragments are detected. The clus-

Table 1
Selected experimental conditions for producing the clusters: c concentration of the molecules in the expansion mix with the carrier gas, T_R and T_0 reservoir and nozzle temperature, respectively, p_0 expansion pressure; and the mean cluster size $\bar{n}$ for conditions, where it was determined.

Carrier gas	Molecule	c (%)	T_R (K)	T_0 (K)	p_0 (bar)	$\bar{n}$
He	Pyrrole	0.3	281	282	1.5	3
	Imidazole	4.1	435	455	2.6	3
	Pyrazole	0.3	333	353	2.0	3
Ar	Pyrrole	0.2	281	282	3.0	Py_nAr_m, $\bar{n} \approx 4$, $\bar{m} \approx 8$
	Imidazole	0.1	377	393	2.5	
		5.4	435	455	2.0	≥6
	Pyrazole	0.5	343	363	2.0	

ters are photoionized by 193.3 nm (6.41 eV) ArF/F_2-Excimer laser. The maximum energy of the 193 nm radiation at the interaction region was about 20 mJ over the 25 ns long laser pulse, corresponding to a photon flux of about 10^{28} cm^{-2} s^{-1}. Alternatively, the clusters can be ionized by electrons with typically 70 eV energy in the following vacuum chamber and the mass spectra of the ionized cluster fragments are then recorded by a quadrupole mass spectrometer.

To determine the mean cluster sizes at various expansion conditions a scattering experiment in a crossed-beam arrangement was performed. The method was originally introduced by Buck and Meyer [25], and it has been employed to determine the mean sizes of various rare gas and molecular clusters, e.g., recently pyrrole clusters have been studied in our lab [9]. Briefly, the skimmed cluster beam is crossed perpendicularly by a beam of He atoms. In elastic collisions the clusters of different sizes are scattered into different laboratory (LAB) angles: in principle the smaller, i.e., lighter, clusters are scattered into the larger angles. By rotating the whole beam source assembly with respect to the rest of the apparatus, the clusters scattered at a particular LAB angle are allowed to proceed to the following vacuum chambers for detection by means of the quadrupole mass spectrometer. By choosing an appropriate scattering angle, clusters *larger* than a certain corresponding size can be excluded from the detection. In addition, the clusters *smaller* than a certain size can be excluded from the detection by selecting an appropriate fragment mass. Thus only clusters from a defined cluster size range are detected. By an analysis of the measured mass spectra and LAB angular distributions for various ionic cluster fragments the mean cluster sizes can be obtained. The complete scattering experiment yielding the fragmentation probabilities of the clusters after ionization includes also measurements of the velocity distributions of the individual ionic fragments at various scattering angles using a pseudo-random chopper (see, e.g., Ref. [26,27]), which is, however, beyond the scope of the present experiment.

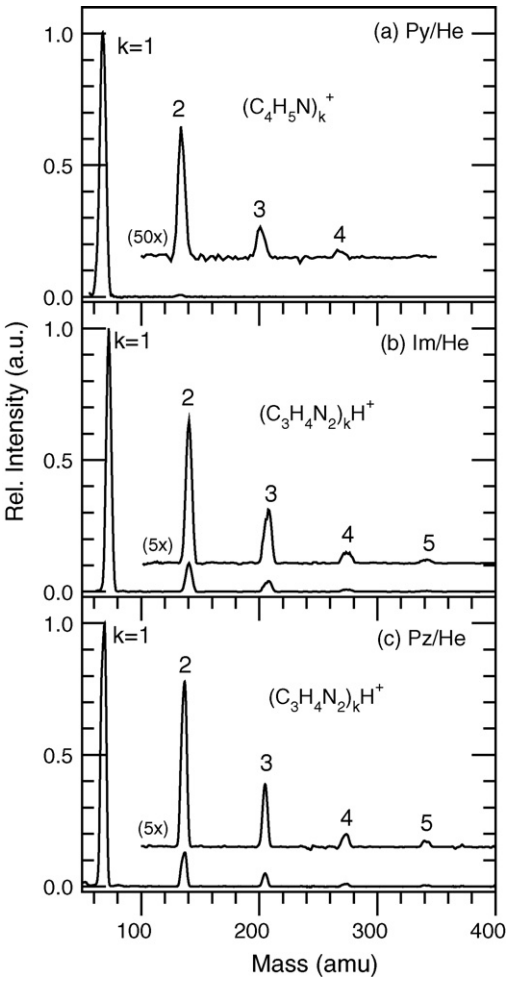

Fig. 3. Quadrupole EI mass spectra of small pyrrole, imidazole and pyrazole clusters produced in coexpansion with He carrier gas. The expansion conditions are summarized in Table 1.

3. Results and discussion

3.1. EI quadrupole mass spectra and cluster size distributions

In this paper we present the results on the electron ionization and photoionization of various clusters of pyrrole, imidazole and pyrazole molecules. Clusters of various sizes – and in case of pyrrole also of various compositions – were produced under different expansion conditions. A range of reservoir T_R and nozzle T_0 temperatures and expansion pressures p_0 was exploited, and different carrier gasses He and Ar were used. Generally, the expansions in He resulted in smaller clusters, while the Ar-expansions resulted in larger species. The cluster size distributions are discussed in this section.

Fig. 3 shows the quadrupole mass spectra of pyrrole, imidazole and pyrazole clusters produced in He expansions. The corresponding expansion conditions are summarized in Table 1. In case of pyrrole the spectrum consists of Py_k^+ molecular cluster fragments, while in case of imidazole and pyrazole the protonated Im_kH^+ and Pz_kH^+ fragments occur. The spectra are dominated by the smallest molecular fragments, i.e., the monomer ion Py^+ and the protonated monomer ions ImH^+ and PzH^+, and decrease exponentially towards larger fragment masses. It should be noted that the focus of the present study is on the ionization of larger clusters rather than molecules, therefore the resolution of our QMS was degraded to achieve a constant transmission over the entire mass region. Yet the exact mass peak maxima positions were obtained from a careful calibration of the spectra together with QMS scans at higher mass resolution. For the calibration, mass spectra of Ar clusters were measured parallel to the present spectra in the entire mass region. A linear regression to the position of the Ar_n^+ mass peak maxima was used to calibrate the mass scale in the spectra of the heterocyclic molecule clusters. This calibration clearly yields the assignment of the observed peak maxima to the Py_k^+ in case of pyrrole and to the protonated species Im_kH^+ and Pz_kH^+ in case of imidazole and pyrazole, respectively. In the view of the limited resolution, the relatively robust assignment of the peak maxima cannot rule out some contributions from other species completely [28]. However, it is also worth noting, that the same fragments occur in the TOFMS spectra (see below), where a sufficiently high resolution could be achieved.

The experimental evidence for the protonated fragments in the case of imidazole and pyrazole clusters vs. pyrrole cluster ions composed of unfragmented molecules is also supported by our *ab initio* calculations. Fig. 4 shows the calculated neutral and ionic structures of the pyrrole, imidazole and pyrazole dimers and the corresponding ions, and outlines the energetics. For comparison, the experimental values of the ionization energies of pyrrole, imidazole and pyrazole molecules are 8.21, 8.81 and 9.38 eV [29], respectively. The different ground state structure of the three species leads to different reaction channels upon ionization. Pyrrole clusters are bound via the N–H$\cdots\pi$ interaction, while the imidazole and pyrazole interaction is mediated by N–H$\cdots$ N hydrogen bonds. Pyrrole clusters behave upon ionization similarly as benzene. Pyrrole dimer forms a stacked structure and the strongly bound dimer

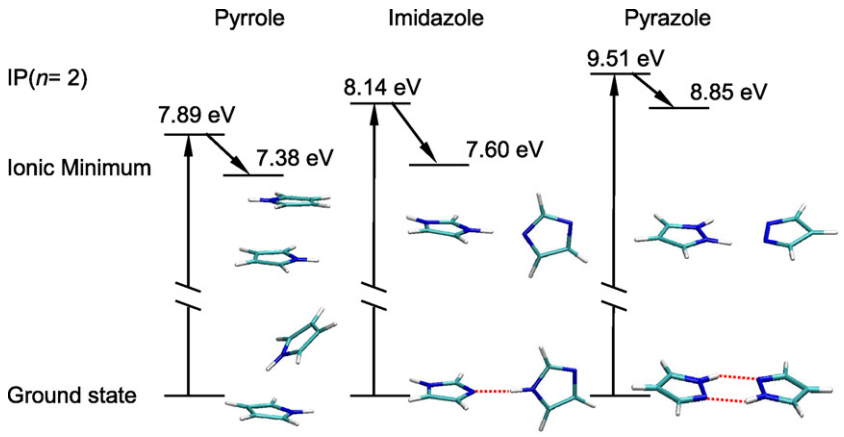

Fig. 4. Structures and energetics of the ionized pyrrole, imidazole and pyrazole dimers calculated at the MP2 level using aug-cc-pVDZ basis set. The upper level IP($n = 2$) for each specie indicates the vertical ionization energy of the corresponding dimer at the equilibrium geometry of the neutral. The ground state neutral geometries are shown at the bottom. The energy levels labeled as ionic minimum correspond to optimized dimer ion structures, which are shown next to it. Thus in case of pyrrole this level is effectively the adiabatic ionization energy, and in case of imidazole and pyrazole these levels correspond to the proton transferred structures as indicated by the depicted geometries.

core is also observed for larger clusters [9]. In the case of imidazole and pyrazole, on the other hand, proton transfer follows the ionization. The proton transfer reaction is observed also for larger clusters.

The mean neutral cluster sizes for conditions corresponding to Fig. 3 were determined in the scattering experiment with the He-atom beam. Detailed results of the scattering experiment with pyrrole clusters have already been presented in Ref. [9]. There the neutral cluster size distribution was derived (see Fig. 6 in Ref. [9]) with the mean cluster size $\bar{n} \approx 3$. For imidazole clusters the scattering experiment has recently been briefly outlined in Ref. [18]. The mean neutral cluster size under these expansion conditions has also been derived as $\bar{n} \approx 3$ [18]. For pyrazole clusters the complete scattering experiment has not been performed, however, the mean neutral cluster size $\bar{n} \approx 3$ can be expected in the view of the similarity between the mass spectra of imidazole and pyrazole clusters in Fig. 3(b) and (c), respectively. This argument is again supported by our *ab initio* calculations. The binding energies per molecule calculated for dimers and trimers (see Fig. 1) were 0.2–0.3 eV for imidazole and 0.3–0.4 eV for pyrazole. Therefore a similar degree of fragmentation can be expected for both systems.

The larger clusters were produced in Ar-expansions. Fig. 5 shows the quadrupole mass spectra of larger pyrrole, imidazole and pyrazole clusters. The corresponding expansion conditions are also summarized in Table 1. Again the scattering experiment was performed to obtain some information about the neutral cluster sizes. The analysis of the scattering experiment for the large pyrrole clusters presented in Ref. [9] led to the conclusion that mixed (or Ar coated) clusters Py_nAr_m were produced with the mean size $\bar{n} \approx 4$ and $\bar{m} \approx 8$. The Ar-coated Py-clusters were also proved spectroscopically by Dauster et al. [30]. The Ar atoms are weakly bound in the clusters and all evaporate in the ionization process as witnessed by the presence of only the Py_k^+ mass peaks in the mass spectra. However, the Ar_m^+ series of peaks was also discernible in the spectra, while in the case of the more strongly bound imidazole and pyrazole clusters only the Ar_2^+ dimer was observed and it disappeared in expansions with higher imidazole and pyrazole concentrations as discussed below (Fig. 6). It should be noted that the mass region of the Py^+ monomer ion at 67 amu and the Ar_2^+ dimer ion at 80 amu was omitted from Fig. 5(a), since both peaks were saturated on this scale, and we focus here on the larger cluster fragments at masses, where the fragments from monomers in the beam do not interfere. In Fig. 5(b) and (c) the spectra start with the protonated fragments ImH^+ and PzH^+, which can originate only from the clusters, i.e., the monomers in the beam do not contribute to these spectra as well. Besides, the angular distribution of the ImH^+ fragment presented below proves that the contribution to this mass peak really comes only from the larger clusters.

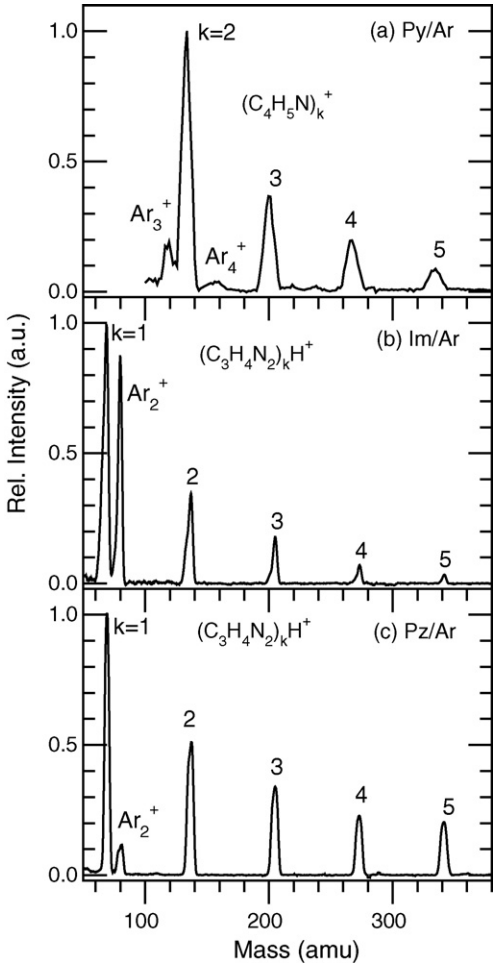

Fig. 5. Quadrupole EI mass spectra of larger pyrrole, imidazole and pyrazole clusters produced in coexpansion with Ar carrier gas. The expansion conditions are summarized in Table 1.

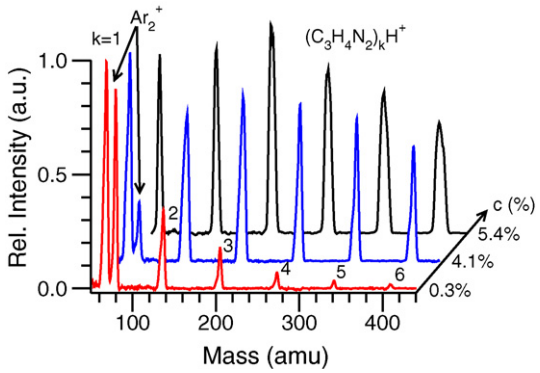

Fig. 6. Dependence of quadrupole EI mass spectra of imidazole clusters produced in coexpansion with Ar on the expansion conditions summarized in Table 1. As the imidazole concentration increases the character of the spectra changes: at the low concentration of 0.3% (red) the mass peak intensities fall off exponentially towards higher masses. At the high concentration of 5.4% (black) the mass peak intensities exhibit a maximum for Im_3H^+. The spectrum at the concentration of 4.1% (blue) represents an intermediate case. Note also that the Ar_2^+ peak disappears with the increasing concentration. (For interpretation of the references to color in this figure legend, the reader is referred to the web version of the article.)

The mass spectrum in Fig. 5(b) was obtained with a low imidazole concentration in Ar of 0.1%. However changing the concentration and expansion conditions the spectra could be changed significantly as illustrated in Fig. 6. The spectrum changes its character from the exponential distribution to a broad distribution with the maximum at a higher Im_kH^+ mass peak ($k = 3$ at the highest concentrations of 5.4%). At the same time the peak corresponding to the argon dimer ion Ar_2^+ disappears with increasing cluster size.

Fig. 7 shows the angular distributions of various Im_kH^+ fragments of Im_n clusters in the scattering with a beam of He atoms. For the smaller clusters generated in He expansions, Fig. 7(a), the ImH^+ fragment extends to the threshold angle for the neutral dimer Im_2. The larger fragments $Im_kH^+ k = 2$ and 3 start to appear approximately at the threshold angles for the neutral tetramer Im_4 and pentamer Im_5, respectively.

Since we focus here on the larger clusters, the scattering experiment for Ar-expansion was performed for the highest imidazole concentration of 5.4% corresponding to the last (black) spectrum in Fig. 6. These angular distributions for Im_kH^+ fragments in Fig. 7(b) exhibit threshold angles corresponding roughly to the neutral Im_n, $n = k + 2$, clusters (again with the exception of $k = 1$ discussed below). This suggests the evaporation of at least two imidazole molecules (without a proton, which has been transferred to the rest of the cluster) in the ionization process. The mean Im_kH^+ ion

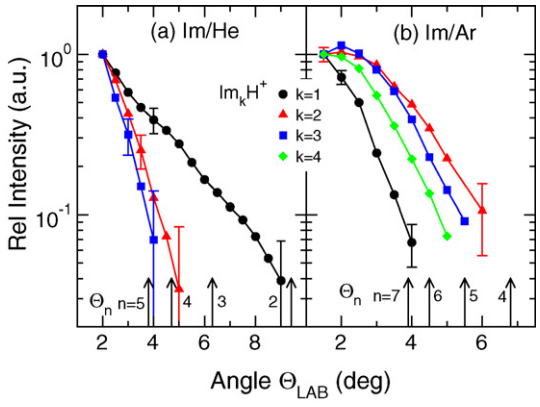

Fig. 7. Angular distribution of imidazole clusters produced in coexpansion with He (a) and Ar (b). Intensities for all masses were normalized to the smallest measured angle.

fragment size from the spectrum in Fig. 6 was determined to be $\bar{k} \approx 4$. Thus the mean neutral Im_n cluster size is at least by 2 larger, i.e., $\bar{n} \geq 6$.

It is also worth noting, that the angular distribution of the protonated monomer ImH^+ fragment in this case falls off very quickly to the threshold angle of $n = 7$ implying that this fragment originates prevailingly from the larger Im_n clusters with $n \geq 7$ and not from the small species such as dimers. Fig. 7(a), on the other hand, indicates that some ImH^+ fragments originate from the smaller clusters, already from the neutral dimers. This can be understood keeping in mind that the He-expansions are dominated by the small clusters. Therefore their contribution to the ImH^+ fragment can be substantial. On the other hand the Ar-expansions are dominated by the larger clusters and the contribution to the ImH^+ fragment from the dimer and other small clusters is probably negligible compared to the contribution from the larger species $n \geq 7$. This suggests that the electron ionization of the larger imidazole clusters can also lead to the evaporation of the protonated ImH^+ ionic fragment from the cluster. Another possibility to explain the origin of the ImH^+ fragment from the large clusters can be double ionization, which is possible with 70 eV electron, and subsequent Coulombic explosion. However, we have measured the mass spectra also at 50 eV, which yielded no significant difference. Although, the double ionization is possible also at 50 eV, its relative importance could be expected to decrease with decreasing electron energy. Therefore we do not expect the Coulombic explosion to have a major effect in the electron ionization process, yet we cannot exclude it completely.

The pyrazole mass spectra follow similar trends with varying the expansion conditions as the imidazole ones, therefore the mean cluster sizes can be expected to be similar. Since we are not interested in the exact cluster sizes here, rather in the general effect, which the clustering has on the ionization process, the scattering experiment was not performed for pyrazole clusters.

3.2. Successive multiphoton ionization

First, we consider the ionization of the small clusters. As mentioned above, the mean cluster size in our beam generated in He-expensions is $\bar{n} \approx 3$. Yet, in the view of the exponential character of the cluster size distribution (see Fig. 6 in Ref. [9]) the population of trimers is only about 45% of the monomer population and the monomers dominate in the molecular beams under these conditions. Therefore a comparison of the present UVMPI TOF spectra to the EI QMS spectra of the molecules can deliver also some information about the ionization mechanisms of the bare molecules. Nevertheless, the focus in the present paper will be on the ionization of the clusters.

Fig. 8 shows the UVMPI TOF mass spectra of the small pyrrole, imidazole and pyrazole clusters. The spectra were measured under the same expansion conditions as the EI QMS spectra presented in Fig. 3. They are summarized in Table 1. The region of the molecular fragments is shown up to 75 amu, since no cluster fragments appeared at higher masses after the photoionization. For comparison the EI QMS spectra of the corresponding molecules are shown (red stick spectra) obtained from the NIST database [29]. We have obtained similar QMS spectra in our experiment, however, a somewhat worse resolution of our quadrupole due to the reasons mentioned above did not allow to resolve the individual peaks as in the mass spectra from Ref. [29]. Therefore we refer to the NIST database spectra [29] for comparison. The proposed assignment of the mass peaks in our UVMPI TOF mass spectra is based on comparison to the photoionization spectra in the literature [5–7], where also the discussion of this assignment can be found, which is, however, not the point here.

Here we concentrate on the differences between the successive multiphoton ionization with 193 nm photons and the electron ion-

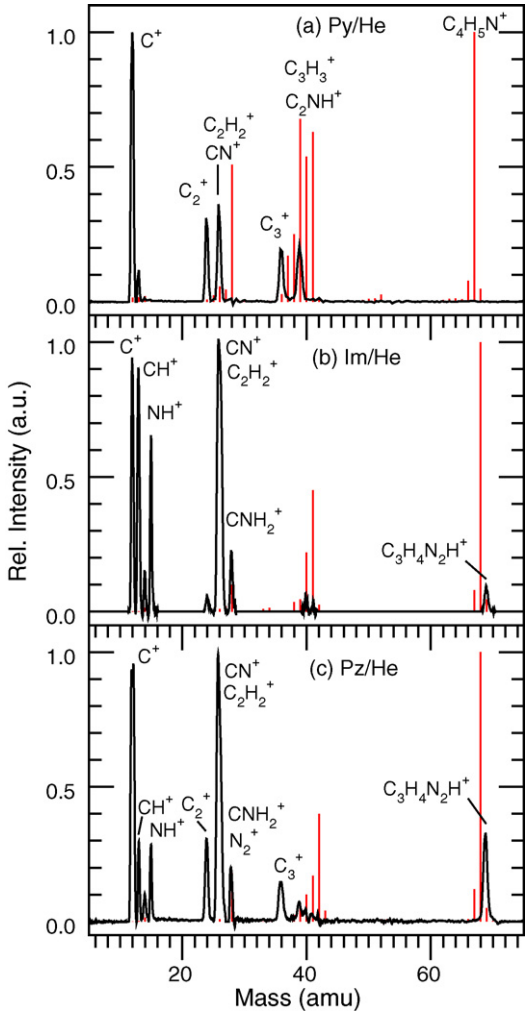

Fig. 8. Photoionization TOF mass spectra of small pyrrole, imidazole and pyrazole clusters produced in coexpansion with He carrier gas. The region of molecular fragments is shown, no fragments appear at higher masses. The expansion conditions are summarized in Table 1 and the photon flux was $\approx 10^{28}$ cm^{-2} s^{-1}. The electron ionization QMS spectra of the corresponding molecules are shown for comparison (red stick spectra) [29]. The mass peak assignments in the TOF spectra are based on the photoionization spectra in the literature [5–7]. (For interpretation of the references to color in this figure legend, the reader is referred to the web version of the article.)

ization with 70 eV electrons. Clearly, the multiphoton ionization leads to significantly higher degree of fragmentation in all three molecules. In particular, the parent molecular ions, which dominate the QMS spectra are not populated at all in the TOF spectra, i.e., the molecule is predominantly fragmented by the successive absorption of two or more photons. It should be noted that the peak at 69 amu in imidazole and pyrazole spectra does not correspond to the parent molecule ion, which would be at 68 amu, but rather to the protonated ImH^+ and PzH^+ ion fragments originating from the clusters. This is also confirmed by the spectra of the larger clusters below, where this peak gains intensity from the larger cluster decomposition.

Further, the EI QMS spectra of all three molecules exhibit a second stronger group of fragments around mass 40 amu, and a weaker peak at 28 amu accompanied by some weak satellites. On the other hand, one of the strongest peaks in all the UVMPI TOF spectra is the smallest fragment C^+ at 12 amu, which is hardly present in the EI QMS spectra. The second strongest fragment peak in the UVMPI TOF spectra of pyrrole and the strongest one in imidazole and pyrazole spectra is the mass of 26 amu ($C_2H_2^+$ and/or CN^+). The group around 40 amu is weaker than the corresponding fragments in the UVMPI TOF spectrum. It is worth noting that the surprisingly strong C^+ peak does not originate from some background hydrocarbon impurities, since the background spectrum is indeed subtracted. A very similar TOFMS spectrum can be found in the literature for pyrrole molecules ionized with 243 nm photons (see Fig. 1 in Ref. [6]). The spectrum in Ref. [6] is also dominated by C^+ and exhibits some contributions from C_2^+ and C_3^+ ions.

On the other hand, the single photon TOFMS spectra of these molecules found in the literature are quite different. For pyrrole these spectra were investigated in great detail at various energies between 12 eV and 28 eV by Rennie et al. [5]. For imidazole Schwell et al. [7] published a single-photon spectra at 21 eV. In general, these spectra exhibit significantly less fragmentation than our present multiphoton spectra. In our experiment the energy corresponding to two-photon absorption is 12.8 eV. The pyrrole spectrum in Ref. [5] at the corresponding single-photon energy of 13 eV is still strongly dominated by the parent ion. Even at the photon energy of 27.55 eV Rennie et al. [5] observed a strong parent peak together with an intense group around mass 40 amu and another strong peak at 28 amu, and only negligible traces of C^+. In the imidazole spectrum at 21 eV the parent peak is weak, however, the group around 40 amu is the strongest and again only very little C^+ is observed [7].

What is the reason for the higher degree of fragmentation in the subsequent non-resonant multiphoton ionization? First, we compare the multiphoton ionization to the electron ionization. Although, the ionizing electron energy of 70 eV is much larger than the 193 nm photon energy (i.e., multiples of 6.4 eV) the energy deposited into the internal excitation of the molecule (cluster) is significantly smaller. It has already been concluded in the literature [31,32], that from the 70 eV electron only an energy of the order of an eV remains as the internal excitation in the molecule after the electron ionization and most of the energy is carried away by the kinetic energy of the two escaping electrons. In particular, for pyrrole clusters we have recently deduced from our experiments [9] that the energy deposited into the internal excitation of the cluster ion was around 1–2 eV.

On the other hand, in the subsequent multiphoton ionization process the energy deposited into the internal excitation of the species can be substantially higher. The photoelectron spectrum of pyrrole following one-colour multiphoton excitation at 243.0 nm in Ref. [6] exhibits a maximum at 0 eV and extends to 2 eV. Even considering only two-photon process a significant portion of the available energy (photon energy minus ionization energy) is deposited into the internal excitation of the molecule. Actually, the appearance of ions such as C^+ in the corresponding mass spectrum in Ref. [6] suggests absorption of more than two photons. Thus in the photoionization process actually more energy can be deposited into the internal excitation of the ion even at lower photon energies.

One important effect, which can lead to the higher degree of fragmentation in the subsequent multiphoton ionization, is the delay between the successively arriving photons. During this delay the species excited with the previous photon can undergo some fragmentation, and the subsequent photon ionizes and/or fragments further the excited species. The cluster can play a role in this process in the way, that it hinders the immediate fragmentation of the species after the absorption of one or several photons. The species can then absorb further photon(s) resulting in highly excited species decaying into small fragments. Whether the species are first fragmented and the fragments subsequently ionized or the species are first ionized and subsequently fall apart cannot be distinguished in the present experiments. We have also recently observed a similar effect in the cluster mediated frustrated photodissociation of acetylene [10].

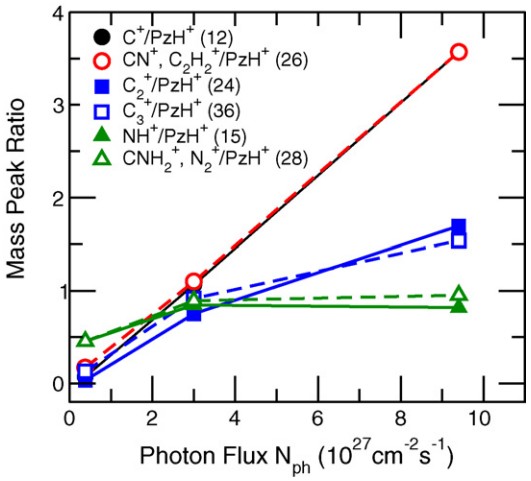

Fig. 9. Intensity ratio between various indicated mass peaks and the PzH^+ peak in the TOFMS of pyrazole clusters as a function of the laser photon flux. Note that the black circles corresponding to the C^+/PzH^+ ratio are blanked out by the open red circles. (For interpretation of the references to color in this figure legend, the reader is referred to the web version of the article.)

To investigate the effect of the delay between the successively absorbed photons and/or the number of absorbed photons, the dependence on the photon flux was measured. Since the signal intensities depend strongly on the photon flux, the multiplier voltage was varied to avoid signal saturation at the stronger mass peaks. It is difficult to reliably normalize the spectra measured at different multiplier voltages. On the other hand the peak intensity ratios are more robust and these values from spectra measured with the different multiplier voltages can still be compared. Therefore in Fig. 9 the ratios of peak intensities are compared rather than the absolute signals. Ratios of various mass peaks to the protonated monomer PzH^+ for pyrazole as a function of the photon flux are plotted. At the small photon fluxes the PzH^+ (originating from the clusters) is the major peak in the spectrum. The peaks at mass 12 amu (C^+) and 26 amu (CN^+ and $C_2H_2{}^+$) dominate the spectrum in Fig. 8(c). These peaks quickly rise with the photon flux. The ratio of the other peaks at 24 amu ($C_2{}^+/PzH^+$) and 36 amu ($C_3{}^+/PzH^+$) also increase, but somewhat slower. On the other hand, e.g., the ratio of the fragments at 15 amu (NH^+/PzH^+) and 28 amu ($CNH_2{}^+$ and/or N_2/PzH^+) increases only very little with the photon flux. We note that, in principle, one could determine how many photon processes contribute to the various mass peaks by fitting their absolute intensity dependence on the photon flux, however, due to the peak intensity saturation effects mentioned above, reliable results could not be obtained.

Nevertheless, some qualitative conclusions can be drawn from the dependencies. The C^+ ion is apparently a product of a large fragmentation caused by a large number of photons, but also the more complex CN^+ and/or $C_2H_2{}^+$ fragments result from the same complete fragmentation. The $C_2{}^+$ and $C_3{}^+$ seem to require somewhat less photons to be created. Finally, the NH^+ and a more complex $CNH_2{}^+$ and/or $N_2{}^+$ fragments roughly follow the dependence of the protonated molecule PzH^+ peak on the photon flux. Thus their generation requires about the same number of photons. It should be also noted, that all the fragments are not necessarily products of a direct ionization and fragmentation process, but the ion-molecular reactions within the ionized cluster can play a role in their generation [33,34]. However, we do not speculate about the possible ion-molecule reactions, which are not the major focus in this paper.

As a final note we cannot determine how many photons were actually absorbed by the species. However, a very rough estimate can be made, assuming a typical absorption cross section of

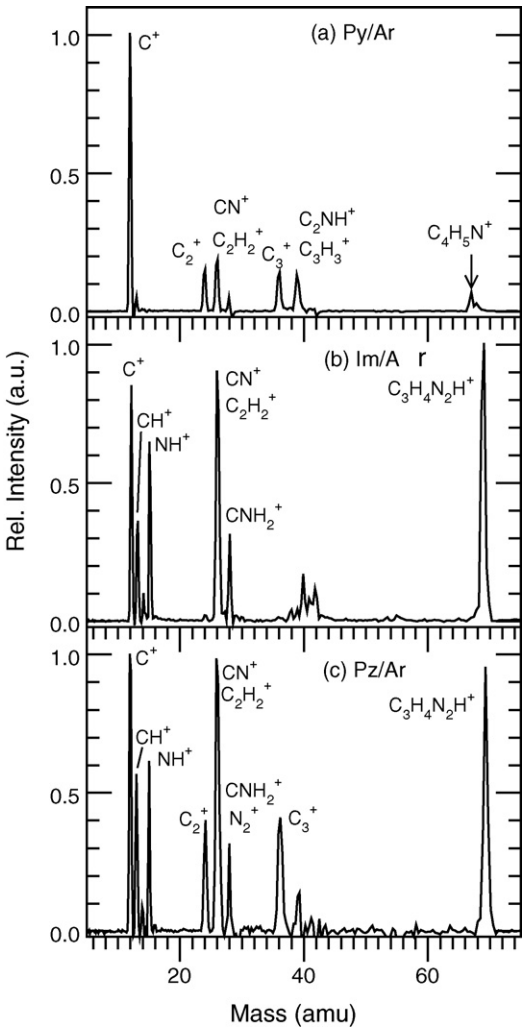

Fig. 10. Photoionization TOF mass spectra of large pyrrole, imidazole and pyrazole clusters produced in coexpansion with Ar. The expansion conditions are summarized in Table 1 and the photon flux was $\approx 10^{28}$ cm^{-2} s^{-1}. The peak assignment as in Fig. 8. Only the part of the spectra with masses smaller than the monomer mass is shown, the parts of the spectra corresponding to the larger cluster fragments is shown in Fig. 11.

10^{-19} cm^2 [35] and a typical photon flux of $\sim 10^{27}$ cm^{-2} s^{-1} during the 25 ns laser pulse duration. Upon the crude assumption that the cross section is not changing with the absorption, about 2–3 photons could be absorbed with a time delay 5–10 ns. In some of the experiments presented here almost ten times higher photon fluxes were employed, which can, indeed, lead to the very high degree of fragmentation. Here the presentation of the results obtained in experiments with the rather high photon fluxes was motivated by the following general question: What photon flux a solvated heterocyclic molecule can survive as integral entity? The present photon fluxes destroy the pyrrole molecule in clusters, while in the hydrogen bonded clusters a fraction of the molecules remains unfragmented, as will be shown below.

Finally, the TOFMS spectra of the larger clusters produced in Ar expansions were measured and summarized in Figs. 10 and 11. The expansion conditions for pyrrole were the same as for the spectrum in Fig. 5(a). For imidazole the expansion of the higher concentration 5.4% mix was employed, and for pyrazole also a mix of about 5% concentration was used. It ought to be mentioned that different expansion conditions were exploited and the various spectra supported the conclusions derived from the selected set of data presented here.

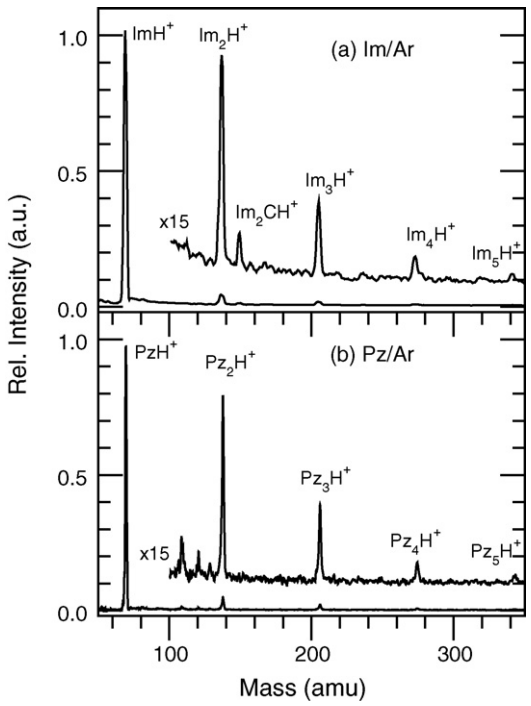

Fig. 11. Photoionization TOF mass spectra of large pyrrole, imidazole and pyrazole clusters produced in coexpansion with Ar. The conditions are the same as in Fig. 10, where the parts of the spectra corresponding to the molecular fragments are shown.

The molecular parts of the spectra up to the mass 75 amu are presented in Fig. 10. They closely resemble the spectra in Fig. 8, however, the major difference is the occurrence of the mass peaks close to the monomer masses. In the pyrrole cluster spectrum a small Py^+ peak occurs accompanied by smaller PyH^+ satellite. On the other hand in the imidazole and pyrazole spectra the corresponding protonated monomers ImH^+ and PzH^+ occur. These peaks appear as the fragments of the larger clusters. The larger cluster fragments can be seen in Fig. 11. In the case of pyrrole almost no fragments larger than the monomer were observed in the UVMPI TOF spectra [36], therefore this spectrum is omitted from Fig. 8. On the other hand imidazole and pyrazole clusters exhibit the larger protonated fragments. As opposed to the QMS, where for the large imidazole clusters the spectrum was dominated by the Im_3H^+ fragment, the TOFMS have exponential character strongly dominated by the protonated monomers. This once again points to the higher degree of cluster fragmentation upon multiphoton ionization. The appearance of the larger cluster fragments in the subsequent multiphoton ionization of imidazole and pyrazole clusters as opposed to the pyrrole clusters points to the stabilization of the former species in the clusters. The hydrogen N–H···N bond in imidazole and pyrazole, which can lead to the hydrogen or proton transfer process upon excitation, seems to stabilize the molecules better than the N–H···π bond in pyrrole clusters.

4. Conclusions

Clusters of pyrrole, imidazole and pyrazole molecules were generated and ionized by electron ionization and a non-resonant subsequent multiphoton process with 193 nm photons. Different clusters size distributions were produced under different expansion conditions and the cluster sizes were analyzed in scattering experiments. Two major issues are discussed in this study: (1) The differences in the methods how are the clusters ionized, i.e., the differences between the non-resonant multiphoton ionization and the single photon and electron ionization. (2) The differences between ionization of pyrrole clusters on one side, and imidazole and pyrazole clusters on the other side.

It has been demonstrated that the non-resonant successive multiphoton ionization leads to a significantly higher degree of fragmentation than either a single-photon or electron ionization. Part of the reason is the energetics. Less energy is deposited into the internal excitation of the system by the ionizing electron than by photons. Although the ionization proceeds with 70 eV electrons, most of the energy above the ionization threshold is carried away in the kinetic energy of the escaping electrons and only a small fraction remains deposited in the internal excitation. For pyrrole clusters this energy was argued to be 1–2 eV [9]. A similar behavior was observed earlier for Ar clusters [31] and for polyatomic hydrocarbon molecules up to heptan [37,38]. On the other hand, at least two 193 nm (6.4 eV) photons necessary for the ionization can possibly leave a somewhat higher excitation energy in the system. And in most cases discussed here probably more than two photons were involved in the ionization–fragmentation process. However, the higher energy cannot be the only reason for the larger fragmentation, since the high energy single-photon ionization found in the literature [5,7] for some of these systems did not yield such a high fragmentation. Thus the time delay between the two successively absorbed photons is suggested to play a role in the fragmentation process. The system undergoes dynamics in the excited state leading to the fragmentation and the already partially fragmented system absorbs the successive photon(s) and is ionized and/or further fragmented. Alternatively, the system is first ionized (by at least two photons) and then undergoes the fragmentation dynamics. The measured dependence on laser photon flux, further underlines the dependence of the fragmentation on the delay between the successively absorbed photons.

The second point here is the difference between ionization of the different clusters. While the pyrrole clusters generate mainly the molecular Py_k^+ fragments, the imidazole and pyrazole spectra are dominated by the protonated Im_kH^+ and Pz_kH^+ fragments. This can be understood in the view of the different bonding motifs in the species. The pyrrole clusters are bound by the weak N–H···π bond, and upon ionization the ionized dimer core is generated, which is solvated by other pyrrole molecules [9]. A similar behavior could be also found for benzene clusters [39]. On the other hand the imidazole and pyrazole clusters pose relatively strong hydrogen bonds N–H···N, which lead to the hydrogen or proton transfer between the cluster constituents upon the excitation.

The existence of the strong protonated monomer fragment and the appearance of the protonated fragments in the imidazole and pyrazole spectra on the one side and their almost complete absence in the pyrrole spectra on the other side, points to the interesting issue of photostability of the hydrogen bonded imidazole and pyrazole clusters. As a result of the multiphoton excitation either the hydrogen atom or the proton is transferred between the molecules, which leads to the energy transfer and dissipation and in this way the protonated species are stabilized by the cluster environment. On the other hand in pyrrole clusters the multiphoton excitation leads to an almost complete decay of the cluster and also of the molecule. Based on the present experimental evidence, we are not able to distinguish between the proton transfer and the H-atom transfer mechanism. However, preliminary molecular dynamics calculations for the imidazole dimer (mentioned also in Ref. [18]) point to the latter process. Further calculations and experiments are currently under way to resolve this issue.

Acknowledgment

Support by the special program “Nanotechnology for society” of the Czech Academy of Sciences via grant Nr. KAN400400651, grants Nr. KJB400400902 and 203/09/0422 of the Grant Agency of the

Czech Republic are acknowledged. O.T. acknowledges the support of student grant by Vakuum Praha, Prague, CZ, and V.P. acknowledges the L'Oréal Fellowship for Women in Science. M.F. acknowledges a special J.E. Purkyně fellowship of the Czech Academy of Sciences and the Alexander von Humboldt Foundation. J.F. acknowledges Marie Curie Intra-European Fellowship No. 235414.

References

[1] T. Ly, R.R. Julian, Angew. Chem. Int. Ed. 48 (2009) 7130.
[2] M. Mine, H. Mori, M. Ogata, S.T.T. Tanaka, E. Miyoshi, Chem. Phys. Lett. 438 (2007) 157.
[3] K. Ohashi, N. Nishi, J. Chem. Phys. 109 (1998) 3971.
[4] P.A. Pieniazek, J. Van de Vondele, P. Jungwirth, A.I. Krylov, S.E. Bradforth, J. Phys. Chem. A 112 (2008) 6159.
[5] E.E. Rennie, C.A.F. Johnson, J.E. Parker, R.F.D.M.P. Holland, D.A. Shaw, Chem. Phys. 250 (1999) 217.
[6] A.J. van den Brom, M. Kapelios, T.N. Kitsopoulos, N.H. Nahler, B. Cronin, M.N.R. Ashfold, Phys. Chem. Chem. Phys. 7 (2005) 892.
[7] M. Schwell, H.-W. Jochims, H. Baumgärtel, S. Leach, Chem. Phys. 353 (2008) 145.
[8] B. Jagoda-Cwiklik, P. Slavíček, L. Cwiklik, D. Nolting, B. Winter, P. Jungwirth, J. Phys. Chem. A 112 (2008) 3499.
[9] V. Profant, V. Poterya, M. Fárník, P. Slavíček, U. Buck, J. Phys. Chem. A 111 (2007) 12477.
[10] M. Fárník, V. Poterya, O. Votava, M. Ončák, P. Slavíček, I. Dauster, U. Buck, J. Phys. Chem. A 113 (2009) 7322.
[11] M.N.R. Ashfold, B. Cronin, A.L. Devine, R.N. Dixon, M.G.D. Nix, Science 312 (2006) 1637.
[12] A.L. Devine, B. Cronin, M.G.D. Nix, M.N.R. Ashfold, J. Chem. Phys. 125 (2006) 184302.
[13] F. Machado, E. Davidson, J. Chem. Phys. 97 (1992) 1881.
[14] L. Serrano-Andres, M. Fulscher, B. Roos, M. Merchan, J. Phys. Chem. 100 (1996) 6484.
[15] M. Su, J. Phys. Chem. A 111 (2007) 1567.
[16] M. Barbatti, H. Lischka, S. Salzmann, C. Marian, J. Chem. Phys. 130 (2009) 034305.
[17] V. Poterya, V. Profant, M. Fárník, P. Slavíček, U. Buck, J. Chem. Phys. 127 (2007) 064307.
[18] V. Poterya, V. Profant, M. Fárník, L. Šištík, P. Slavíček, U. Buck, J. Phys. Chem. A 113 (2009) 14583.
[19] R. Baumfalk, U. Buck, C. Frischkorn, S.R. Gandhi, C. Lauenstein, Ber. Bunsenges. Phys. Chem. 101 (1997) 606.
[20] U. Buck, J. Phys. Chem. A 106 (2002) 10049.
[21] P. Slavíček, P. Jungwirth, M. Lewerenz, N.H. Nahler, M. Fárník, U. Buck, J. Chem. Phys. 120 (2004) 4498.
[22] M. Fárník, N.H. Nahler, U. Buck, P. Slavíček, P. Jungwirth, Chem. Phys. 315 (2005) 161.
[23] C. Eon, C. Pommier, G. Guiochon, J. Chem. Eng. Data 16 (1971) 408.
[24] P. Jiménez, M.V. Roux, C. Turrión, F. Gomis, J. Chem. Thermodyn. 19 (1987) 985.
[25] U. Buck, H. Meyer, Phys. Rev. Lett. 52 (1984) 109.
[26] U. Buck, H. Meyer, J. Chem. Phys. 84 (1986) 4854.
[27] U. Buck, J. Phys. Chem. 92 (1988) 1023.
[28] It should be noted, that the different resolution of different QMS mass spectra was caused by exchanging some electronic parts in our QMS system during the long time span of our experiments (more than 2 years). However, this did not influence the general results, since the transmission calibration was always performed with Ar-clusters to keep the transmission in the cluster mass region constant.
[29] In NIST Mass Spec Data Center, S.E. Stein, director, "Mass Spectra" in NIST Chemistry WebBook, NIST Standard Reference Database Number 69; P.J. Linstrom, W.G. Mallard (Eds.), National Institute of Standards and Technology, Gaithersburg, MD, 20899 (http://webbook.nist.gov), June 2005.
[30] I. Dauster, C.A. Rice, P. Zielke, M.A. Suhm, Phys. Chem. Chem. Phys. 10 (2008) 2827.
[31] P. Lohbrandt, R. Galonska, H.J. Kim, M.S.C. Lauenstein, U. Buck, Atomic and molecular beams, in: R. Campargue (Ed.), The State of the Art 2000, Springer, Berlin, 2001, p. 623.
[32] V. Poterya, M. Fárník, U. Buck, D. Bonhommeau, N. Halberstadt, Int. J. Mass Spectrom. 280 (2009) 78.
[33] U. Buck, C. Lauenstein, H. Meyer, R. Sroka, J. Phys. Chem. (1916) 92.
[34] U. Buck, M. Hobein, R. Krohne, H. Linnartz, Z. Phys. D 20 (1991) 181.
[35] In Ref. [18] we observe multiphoton photodissociation of imidazole clusters and conclude that the absorption cross section would have to be larger than 4×10^{-20} cm^2 in order to observe this process. In addition, from the relative cross section measured in Ref. [12] it follows that the cross section at 193 nm is more than 10× larger than at 243 nm. Therefore it is probably larger than the assumed 10^{-19} cm^2.
[36] A small dimer ion Py_2^+ peak could be recognized in the spectrum upon large magnification.
[37] W.A. Chupka, M. Kaminsky, J. Chem. Phys. (1991) 35.
[38] H. Ehrhardt, F. Linder, Z. Naturforsch. 22a (1967) 444.
[39] M.J. Rusyniak, Y.M. Ibrahim, D.L. Wright, S.N. Khanna, M.S. El-Shall, J. Am. Chem. Soc. 125 (2003) 12001.